



## SEISMIC RISK ASSESSMENT OF SPATIALLY DISTRIBUTED STRUCTURES

K. Goda<sup>1</sup> and H.P. Hong<sup>2</sup>

### ABSTRACT

Simultaneous damage of structures and infrastructure due to large earthquakes can be catastrophic for modern society. The simultaneous damage of many structures is spatially correlated since earthquake excitations are originated from the same source. However, earthquake excitations do vary from location to location. This variability consists of earthquake-to-earthquake (inter-event) variability and site-to-site (intra-event) variability; the former can be characterized by the correlation of response spectra at different vibration periods, whereas the latter can be mostly characterized by the spatial correlation. This study investigates the impact of the correlation of seismic demand on the quantitative seismic risk assessment of a group of spatially distributed structures. The results of such an investigation can be of particular importance for corporate managers, city planners, and insurers who face with potential seismic risk for a group of spatially distributed structures in their jurisdictions. For the seismic risk assessment, a building inventory that mimics a typically observed one in western Canada is employed. The analysis results suggest that the impact of the correlation of seismic demand can be significant depending on characteristics of the considered building inventory. It is noted that the expected seismic loss is the same whether the correlation of seismic demand is considered or ignored, whereas the probability distribution function of the aggregate seismic losses can be very different. Consequently, the probability of exceeding a specified aggregate seismic loss level could be significantly different.

### Introduction

Infrequent but large earthquakes can cause severe damage to buildings and infrastructure. Adequate protection against potentially catastrophic seismic excitations can be achieved through implementation of judiciously stipulated seismic provisions in design codes whereas additional protection can be obtained through risk mitigation measures and earthquake insurance (Kleindorfer et al. 2005). To make sound and effective decisions in managing seismic risk, it is necessary to quantitatively and accurately evaluate seismic risk at stake. In dealing with catastrophic seismic risk, one must use the probabilistic characterizations of seismic demand, nonlinear structural response, and structural resistance. One of the most popular tools that have been employed in the literature is the HAZUS-MH (FEMA and NIBS 2003).

It is noted that the HAZUS-MH adopts a fragility-based approach for damage assessment by comparing inelastic demand spectrum and nonlinear capacity curve, and calculates average seismic losses for a given scenario earthquake. The latter can be relaxed by considering multiple scenario earthquakes with their occurrence probabilities rather than a single event (Grossi 2000). It is also noted that earthquake excitations are spatially correlated. The spatial correlation affects the probabilistic characterization of the

---

<sup>1</sup>Ph.D. candidate, Dept. of Civil & Environmental Engineering, University of Western Ontario, London, ON N6A 5B9

<sup>2</sup>Professor, Dept. of Civil & Environmental Engineering, University of Western Ontario, London, ON N6A 5B9

number of damaged structures and the aggregate damage losses for multiple buildings (Hong 2000; Wesson and Perkins 2001; Bazzurro and Luco 2004; Bommer and Crowley 2006). However, this fact is not incorporated in the current HAZUS-MH model.

In the present study, the spatial correlation of seismic excitations due to intra-event and inter-event variability is considered for seismic risk assessment, and a framework to assess the probability distribution of seismic losses for spatially distributed structures is developed. The advantage and novelty of the proposed framework include: 1) a simple simulation technique is adopted, which can deal with Poisson and non-Poisson earthquake occurrence models; 2) statistical characteristics of spatially correlated seismic excitations are incorporated according to their sources since they affect seismic risk for a group of structures in a different manner; 3) damage assessment is carried out directly based on the concept of the reliability theory and the limit state design format; and 4) simulated samples of seismic losses can be used for evaluating the statistics of detailed grouped/ungrouped loss quantities which could be especially important for financial and insurance applications. Although in the developed framework a structure is approximated by a bilinear single-degree-of-freedom (SDOF) system, this can be improved by incorporating detailed nonlinear structural modeling in the future. As will be shown, the framework promotes not only scenario earthquake analyses but also provides present value analyses of the seismic losses for a group of structures during the service period. The salient features of the developed seismic risk assessment framework, which is tailored for western Canadian environment, are succinctly summarized in the following. A numerical example is used to demonstrate and to highlight, in particular, effects of the correlation of seismic demand on the aggregate seismic losses for a group of spatially distributed structures located in a relatively small area. Further, implications of the results on efficient seismic risk management are discussed.

## **Seismic Risk Model for a Group of Structures**

### **Seismic Hazard Modeling**

#### ***Synthetic Earthquake Catalog***

Probabilistic characterizations of seismic hazard can be achieved by combining earthquake occurrence models, seismic source zones, magnitude-recurrence relations, and attenuation relations through the total probability theorem. By adopting the seismic hazard model developed by Adams and Halchuk (2003), which is the basis for the seismic provisions of the 2005 National Building Code of Canada (NBCC, NRCC 2005), a synthetic earthquake catalog can be constructed (Goda and Hong 2006; Hong et al. 2006). For example, if the regional seismic source model for western Canada illustrated in Fig. 1a (Adams and Halchuk 2003) is employed, earthquake events over a long duration can be simulated considering both aleatory and epistemic uncertainty, and relevant seismic event information such as the occurrence time, earthquake magnitude, and earthquake location is stored. It is noted that non-stationary or time-dependent earthquake occurrence processes which are of particular interest for the Cascadia subduction events, can be easily incorporated in simulation.

#### ***Strong Ground Motion Attenuation Relation and Spatial Correlation***

For a given seismic event, ground motion parameters such as the peak structural responses of a linear elastic SDOF system can be predicted using empirical attenuation relations. In this study, the pseudo-spectral acceleration (PSA) for the fundamental vibration period  $T_n$  and damping ratio  $\xi$ ,  $S_{AE}(T_n, \xi)$ , is adopted as an intensity measure since it presents a better predictive power of incurred structural damage over other conventional intensity measures such as the Modified Mercalli Intensity (MMI) and the peak ground acceleration (PGA).

A typical empirical attenuation relation can be expressed as,

$$\ln S_{AE}(T_n, \xi) = f(M, D, \theta) + \varepsilon, \quad (1)$$

where  $f(M, D, \theta)$  is a function of the earthquake magnitude  $M$ , distance  $D$ , and other explanatory variables  $\theta$ , and  $\varepsilon$  represents an error term including both intra-event and inter-event variability and is often assumed to

be normally distributed with a mean equal to zero and a standard deviation equal to  $\sigma_T$ . For shallow crustal earthquakes and interface/inslab subduction earthquakes in western Canada, Adams and Halchuk (2003) adopted the attenuation relation by Boore et al. (1993) and that by Youngs et al. (1997), respectively. This study adopts these relations as well as newly developed relations: the relation developed by Atkinson and Boore (2003) for subduction earthquakes and the relation developed by Hong and Goda (2007) for shallow earthquakes. The latter sets of relations are included for a comparative purpose.

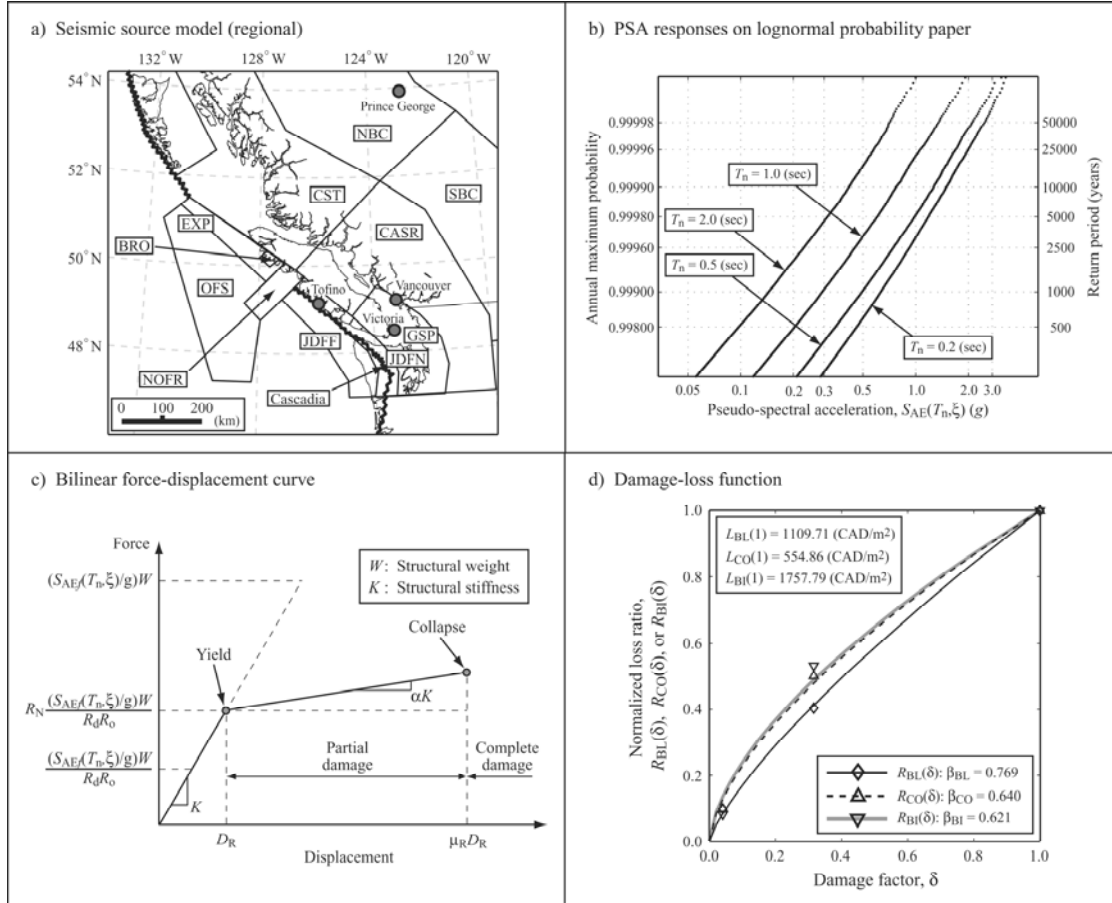


Figure 1. Components of the developed seismic risk model.

To adequately capture catastrophic seismic losses and to extend existing seismic hazard and risk assessment methodologies for a single structure to those for multiple structures, the spatial correlation of seismic demand needs to be considered (Bazzurro and Luco 2004; Bommer and Crowley 2006). To incorporate the spatial correlation, we note that the normal variate  $\varepsilon$  with a variance  $\sigma_T^2$  can be calculated from the variance due to the inter-event variability  $\sigma_1^2$  and the variance due to the intra-event variability  $\sigma_2^2$ , resulting in  $\sigma_T^2 = \sigma_1^2 + \sigma_2^2$ . Based on the studies carried out by Boore (1997), Wesson and Perkins (2001), Kawakami and Mogi (2003), Wang and Takada (2005), and Baker and Cornell (2006), and the analysis results of more than 500 California records, Goda and Hong (2007) suggested that the following equation to predict the correlation coefficient of  $\ln(S_{AE}(T_n, \xi))$  (i.e.,  $\varepsilon$ ),  $\rho(T_{n1}, T_{n2}, \Delta_{12})$ , could be used for seismic hazard and risk assessments,

$$\rho(T_{n1}, T_{n2}, \Delta_{12}) = \frac{\rho_1(T_{n1}, T_{n2})(\sigma_1(T_{n1})\sigma_1(T_{n2})) + \rho_2(\Delta_{12}, \max(T_{n1}, T_{n2}))\sigma_2(T_{n1})\sigma_2(T_{n2}))}{\sigma_T(T_{n1})\sigma_T(T_{n2})}, \quad (2)$$

where  $T_{n1}$  and  $T_{n2}$  represent the natural vibration periods of the SDOF systems at two sites separated by a distance of  $\Delta_{12}$ ,  $\rho_1(T_{n1}, T_{n2})$  represents the correlation coefficient suggested by Baker and Cornell (2006) for

$\Delta_{12} = 0$ , and the relation for  $\rho_2(\Delta_{12}, \max(T_{n1}, T_{n2}))$  is given by (Goda and Hong 2007),

$$\rho_2(\Delta_{12}, \max(T_{n1}, T_{n2})) = \exp(-\eta_1(\Delta_{12})^{\eta_2}), \quad (3)$$

in which  $\eta_1$  and  $\eta_2$  are the model parameters that are given as follows,

$$\eta_1 = -0.16 \ln(\max(T_{n1}, T_{n2})) + 0.68, \text{ and } \eta_2 = 0.44. \quad (4)$$

Therefore, if the spatial correlation is considered, the evaluation or simulation of the PSA responses at different sites depends on a set of correlated normal variates  $\varepsilon_i$ ,  $i = 1, \dots, m$ , for each seismic event with the correlation coefficient matrix defined by Eqs. 2, 3, and 4. An illustration of the simulated samples of the PSA responses for several vibration periods that are plotted on lognormal probability paper, is shown in Fig. 1b. The results suggest that the PSA responses could be modeled as a lognormal variate. Note that the probability distribution shown in Fig. 1b can be used to develop uniform hazard spectra and to evaluate fractiles corresponding to an adopted probability level for seismic design.

## Damage Assessment and Seismic Loss Estimation

### Reliability-based Damage Assessment

Structures subject to severe ground shakings exhibit nonlinear structural behavior and suffer from occasional damage and collapse. For a structure with the yield displacement capacity  $D_R$  and the displacement ductility capacity  $\mu_R$ , which is approximated by a bilinear SDOF system (see Fig. 1c) and is subjected to the seismic excitation of the  $j$ -th synthetic earthquake event with the PSA equal to  $S_{AEj}(T_n, \xi)$ , the structural damage could be represented by the damage factor  $\delta_j$  as,

$$\delta_j = \min((\mu_{Dj} D_R - D_R) / (\mu_R D_R - D_R), 1) = \min((\mu_{Dj} - 1) / (\mu_R - 1), 1), \quad (5)$$

for  $S_{DEj}(T_n, \xi) = (T_n / (2\pi))^2 S_{AEj}(T_n, \xi) \geq D_R$ , where  $\mu_{Dj}$  is the displacement ductility demand due to the  $j$ -th event. For evaluating the probability of incipient damage level  $\delta_j$ , the limit state function  $g$  defining the specified ductility demand  $\mu_{Dj}$ , that has been just exceeded, is given by,

$$g = \mu_{Dj} / \mu(T_n, \xi, \alpha, \zeta) - 1, \quad (6)$$

where  $\mu(T_n, \xi, \alpha, \zeta)$  is a Frechet variate and represents the ductility demand for a bilinear SDOF system with the post-yield to initial stiffness ratio  $\alpha$  and the normalized yield displacement  $\zeta = D_R / S_{DEj}(T_n, \xi)$  (Hong and Hong 2006). Thus, for the  $i$ -th structure, given the samples of structural capacity  $\mu_{Ri}$  and  $D_{Ri}$ , and seismic demand  $S_{AEij}(T_n, \xi)$ ,  $\mu(T_n, \xi, \alpha, \zeta)$  is obtained by solving  $g = 0$  in Eq. 6, and the damage factor  $\delta_{ij}$  due to the  $j$ -th earthquake is calculated using Eq. 5.

To associate the simplified representation of the structural capacity with the 2005 NBCC seismic design format (NRCC 2005), we note that the minimum required design base shear force  $V_d$  equals  $(S_{AE}(T_n, \xi) / g) M_v / I_E W / (R_d R_o)$  where  $S_{AE}(T_n, \xi)$  is the design spectral acceleration including site modification factors,  $M_v$  is the factor accounting for higher mode effects,  $I_E$  is the importance factor,  $W$  is the total weight of the structure,  $R_d$  is the ductility-related force modification factor, and  $R_o$  is the overstrength-related force modification factor. Note that the actual yield capacity of a designed structure differs from  $V_d$ . This difference and the ratio between the former and the latter denoted by  $R_N$  are illustrated in Fig. 1c.

### Seismic Loss Estimation

It is a demanding task to relate damage measures to incurred losses for a variety of structural systems, material types, categories of service provided by the structure, and construction practices at different locations and times. We note that extensive information on the damage cost and its corresponding damage state ( $ds$ ) represented by the median maximum interstory drift ratio  $\Delta_{ID}(ds)$  is given in the HAZUS-MH. In this study, the preceding damage factor  $\delta$  for the damage state  $ds$ , denoted by  $\delta(ds)$ , is

considered to be related to  $\Delta_{ID}(ds)$  by,

$$\delta(ds) = \frac{\Delta_{ID}(ds) - (\Delta_{ID}(slight) + \Delta_{ID}(moderate))/2}{\Delta_{ID}(complete) - (\Delta_{ID}(slight) + \Delta_{ID}(moderate))/2} \quad (7)$$

where  $ds$  is described as *none*, *slight*, *moderate*, *extensive*, and *complete* in the HAZUS-MH. This definition is guided by FEMA and NIBS (2003) and Barbat et al. (2006). In the HAZUS-MH loss estimation methodology, a fraction of the damage cost in the “complete” damage state is associated with the damage costs in partial damage states. The seismic losses of a building for a given  $ds$  is conveniently categorized into three types: building-related loss  $L_{BL}(ds)$ , content-related loss  $L_{CO}(ds)$ , and business-interruption-related loss  $L_{BI}(ds)$  whose replacement values are expressed as  $L_{BL}(1)$ ,  $L_{CO}(1)$ , and  $L_{BI}(1)$ , respectively. Based on these and using the information given in the HAZUS-MH database, one can calculate the normalized loss ratios  $R_{BL}(ds) = L_{BL}(ds)/L_{BL}(1)$ ,  $R_{CO}(ds) = L_{CO}(ds)/L_{CO}(1)$ , and  $R_{BI}(ds) = L_{BI}(ds)/L_{BI}(1)$  for different structural types and occupancy types, and express these in terms of the damage factor  $\delta$  with the help of Eq. 7. An illustration of the obtained normalized loss ratios is shown in Fig. 1d for a concrete shear wall structure for professional/technical/business service category. Note that the values of  $L_{BL}(1)$ ,  $L_{CO}(1)$ , and  $L_{BI}(1)$  shown in Fig. 1d are calculated by using the unit costs suggested in the HAZUS-MH database but adjusted to 2003 Canadian dollars (CAD) for Vancouver according to the information given in Means (2003). Note also that each ratio shown in the figure could be approximated by a power function as,

$$R_{BL}(\delta) = \delta^{\beta_{BL}}, \quad R_{CO}(\delta) = \delta^{\beta_{CO}}, \quad \text{and} \quad R_{BI}(\delta) = \delta^{\beta_{BI}}, \quad (8)$$

where  $\beta_{BL}$ ,  $\beta_{CO}$ , and  $\beta_{BI}$  are the fitted model parameters.

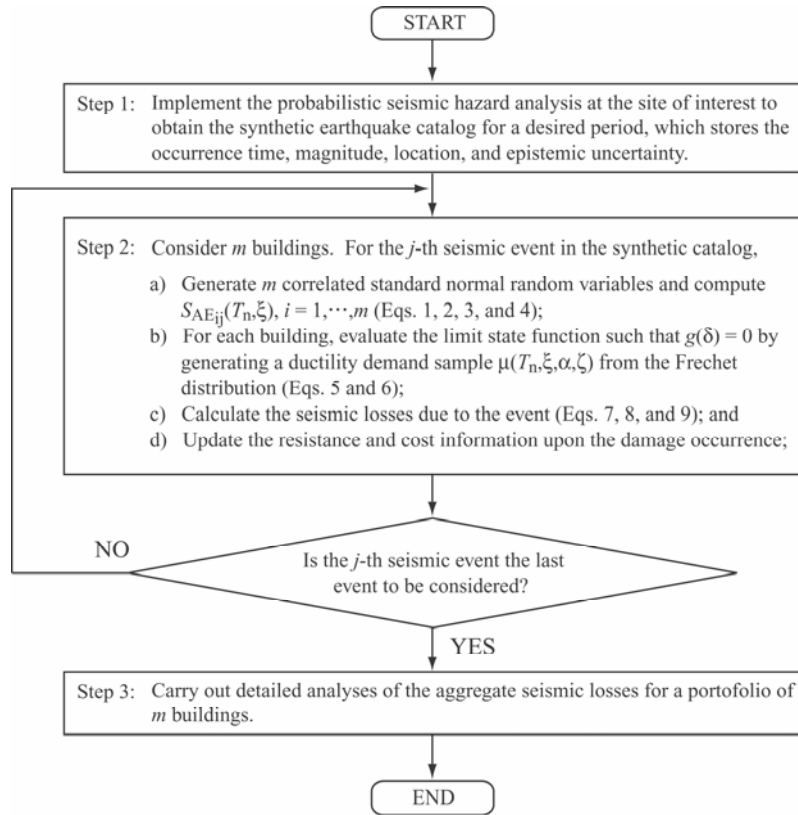


Figure 2. Simulation flowchart.

Based on the preceding, the discounted aggregate seismic losses  $L_A(t, \gamma)$  for  $m$  structures that experience  $n(t)$  seismic events occurring at time  $\tau_j$ ,  $j = 1, \dots, n(t)$  over a fixed duration  $t$ , can be expressed as,

$$L_A(t, \gamma) = \sum_{j=1}^{n(t)} \sum_{i=1}^m (L_{BL}(\delta_{ij}) + L_{CO}(\delta_{ij}) + L_{BI}(\delta_{ij})) \exp(-\gamma \tau_j), \quad (9)$$

where  $\gamma$  is the discount rate. This expression is flexible to accommodate various loss quantities by selecting different values of  $t$  and  $\gamma$ . The steps for evaluating  $L_A(t, \gamma)$  by using the simulation technique is shown in Fig. 2. In simulation, damaged or collapsed structures are assumed to be restored immediately to their original conditions.

## Impact of Correlated Seismic Excitations on Aggregate Seismic Losses

### Seismic Hazard Scenario and Building Inventory

To illustrate the applicability of the proposed seismic risk assessment framework, and to investigate the impact of the spatial correlation of seismic demand on the estimated seismic losses, a group of 200 hypothetical buildings located in Vancouver (49.2°N, 123.2°W) is considered. The group of buildings is subject to the seismic hazard represented by the regional model presented in Fig. 1a. The Cascadia subduction events are considered as a Poisson process with a characteristic magnitude of 8.2 and a recurrence period of 600 years (Adams and Halchuk 2003). For seismic hazard and risk assessments, two sets of attenuation relations, Set-1 and Set-2, are employed: Set-1 includes the attenuation relations adopted by Adams and Halchuk (2003) for developing the seismic hazard maps of Canada, and Set-2 includes those developed by Atkinson and Boore (2003) for subduction earthquakes, and by Hong and Goda (2007) for shallow earthquakes. Further, it is considered that the spatial correlation coefficients shown in Eqs. 2, 3, and 4 are equally applicable to all the considered attenuation relations. The local site condition for buildings is the site class C (NRCC 2005) whose shear wave velocity in the uppermost 30 m,  $V_{s30}$ , is considered to be 555 m/s.

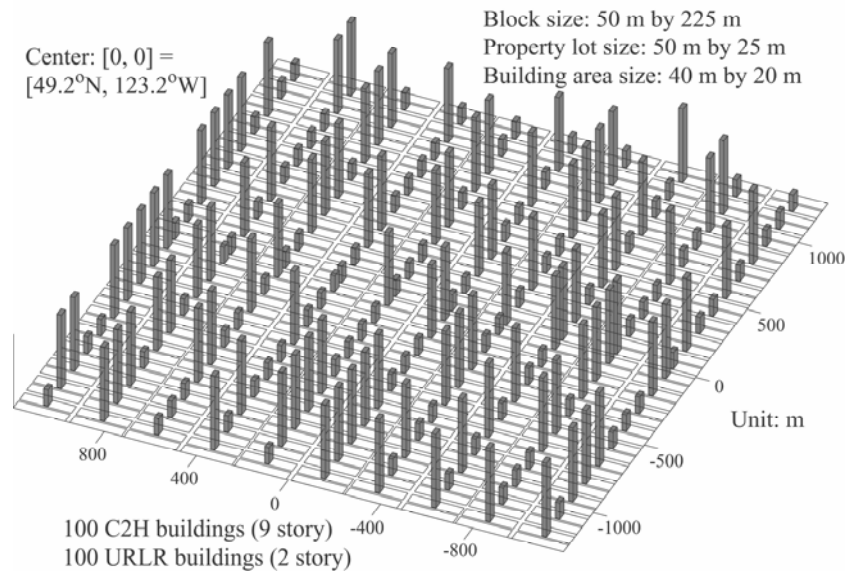


Figure 3. Spatially distributed buildings.

The hypothetical building inventory comprises 100 high-rise concrete shear walls structures (C2H according to the HAZUS-MH classification) for commercial use (COM4 according to the HAZUS-MH classification) and 100 low-rise unreinforced masonry bearing walls structures (URML according to the

HAZUS-MH classification) for commercial use (COM1 according to the HAZUS-MH classification). These buildings are distributed uniformly over a 2.5 km by 2.5 km area as illustrated in Fig. 3. For the same structural type, the identical statistical information on the structural capacity, design property, and damage cost shown in Table 1 is considered. The selection of the statistics shown in Table 1 is guided by the information given in Munich Re. (1992), Onur et al. (2005), FEMA and NIBS (2003), and NRCC (2005). All the cost information is adjusted to 2003 CAD for Vancouver according to the information given in Means (2003). The design spectral acceleration values  $S_{AEf}$  shown in Table 1 represent the estimated 2% in 50 years return period values of the PSA, which are based on the unconditional fractile (i.e., mean estimate) rather than the median estimate that is adopted in the 2005 NBCC (NRCC 2005). For the seismic risk assessment, both sets of attenuation relations (i.e., Set-1 and Set-2) are considered.

Table 1. Structural capacity, design, and damage cost information of the considered building inventory.

Structural type	Structural capacity & cost information	Structural design information
Concrete shear walls	HAZUS-MH structural & occupancy types: C2H & COM4; 9 story; Building area size: 40 m by 20 m; $T_n = 1.1$ (s); $\mu_R \in \text{LN}(4.0, 0.5)^*$ ; $R_N \in \text{LN}(2.5, 0.15)$ ; $L_{BL}(1) = 1109.71$ (CAD/m <sup>2</sup> ); $L_{CO}(1) = 554.86$ (CAD/m <sup>2</sup> ); $L_{BI}(1) = 1757.79$ (CAD/m <sup>2</sup> ); $\beta_{BL} = 0.769$ ; $\beta_{CO} = 0.640$ ; $\beta_{BI} = 0.621$ ; $\gamma = 0.05$ .	$M_v = I_E = 1.0$ ; Concrete ductile shear walls: $R_d = 3.5$ ; $R_o = 1.6$ ; $S_{AEf} = 0.438$ (g) based on Set-1; $S_{AEf} = 0.417$ (g) based on Set 2.
Unreinforced masonry bearing walls	HAZUS-MH structural & occupancy types: URML & COM1; 2 story; Building area size: 40 m by 20 m; $T_n = 0.4$ (s); $\mu_R \in \text{LN}(2.0, 0.5)$ ; $R_N \in \text{LN}(1.5, 0.15)$ ; $L_{BL}(1) = 512.18$ (CAD/m <sup>2</sup> ); $L_{CO}(1) = 283.87$ (CAD/m <sup>2</sup> ); $L_{BI}(1) = 256.38$ (CAD/m <sup>2</sup> ); $\beta_{BL} = 0.810$ ; $\beta_{CO} = 0.687$ ; $\beta_{BI} = 0.434$ ; $\gamma = 0.05$ .	$M_v = I_E = 1.0$ ; Masonry shear walls: $R_d = 1.5$ ; $R_o = 1.5$ ; $S_{AEf} = 1.109$ (g) based on Set-1; $S_{AEf} = 0.864$ (g) based on Set-2.

\* $X \in \text{LN}(m, v)$  represents that  $X$  is lognormally distributed with a mean equal to  $m$  and coefficient of variation equal to  $v$ .

### Impact of Spatially Correlated Seismic Demand

To focus on the sensitivity analysis of aggregate seismic losses due to spatially correlated seismic excitations, uncertainty in local soil conditions (i.e.,  $V_{s30}$ ) and cost information, and correlation of structural capacity and cost information among buildings are ignored. Note that seismic losses due to casualty are not included. For the sensitivity analysis, three cases, namely, no correlation, full correlation, and partial correlation based on Eqs. 2, 3, and 4, are considered. Based on the above information and using the proposed seismic risk analysis framework, the obtained samples of the aggregate seismic losses  $L_A(t, \gamma)$  for  $t = 50$  years with a simulation cycle of 10,000 are plotted on the Gumbel probability paper in Fig. 4, and the statistics of  $L_A(t, \gamma)$  are shown in Table 2. For the results shown in Fig. 4, the Set-1 attenuation relations are employed.

The results presented in Fig. 4 suggest that the probability distribution functions of  $L_A(t, \gamma)$  have different slopes and intersect one another around the 50-year probability level of 0.94. The probability distribution function obtained by considering realistic spatial correlation of seismic demand lies between those obtained with no correlation and full correlation. In other words, as the spatial correlation increases, the probability of no seismic loss and the probability of extremely large seismic losses increase drastically. Therefore, the consideration of the realistic spatial correlation of seismic demand can be very important in assessing the probability distribution of  $L_A(t, \gamma)$ . Fig. 4 also suggests that the probability distribution of  $L_A(t, \gamma)$  can be approximated by a Gumbel variate in the upper tail region.

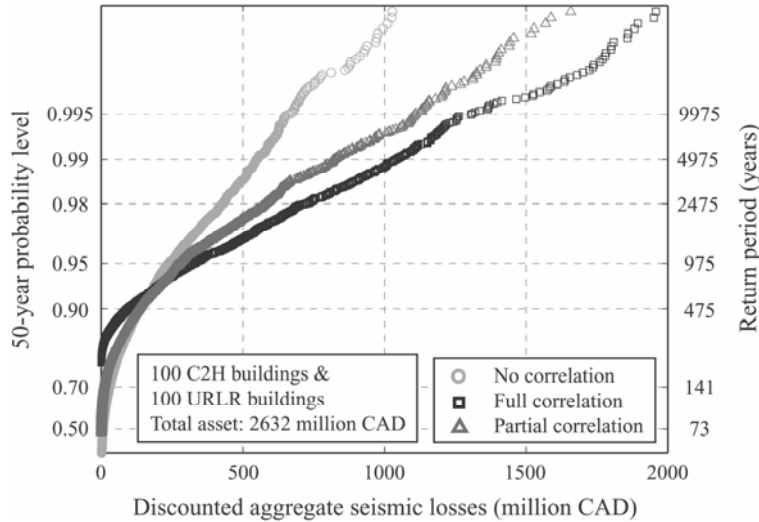


Figure 4. Discounted 50-year aggregate seismic losses plotted on the Gumbel probability paper (attenuation relations in Set-1 are adopted).

Table 2. Statistics of the aggregate seismic losses.

Statistics	No correlation	Full correlation	Partial correlation
Probability of no seismic loss in 50 years	0.275*, [0.420]**	0.783, [0.823]	0.480, [0.601]
Mean & standard deviation of discounted 50-year aggregate seismic losses (million CAD)	48.1 & 112.4, [41.8 & 116.9]	50.3 & 193.9, [42.8 & 181.9]	50.2 & 156.9, [42.7 & 156.6]
Fractile value at 0.80 level (million CAD)	59.0, [38.1]	1.0, [0.0]	36.0, [15.0]
Fractile value at 0.90 level (million CAD)	139.1, [115.3]	94.7, [48.8]	131.0, [93.9]
Fractile value at 0.95 level (million CAD)	240.2, [237.8]	328.6, [265.9]	276.7, [246.3]
Fractile value at 0.98 level (million CAD)	431.5, [431.3]	726.3, [699.5]	579.0, [518.8]

\*Values are based on the attenuation relations in Set-1; \*\*Values are based on the attenuation relations in Set-2.

The results shown in Table 2 indicate that the mean value of  $L_A(t, \gamma)$  is almost the same for the considered three correlation cases whereas the standard deviation of  $L_A(t, \gamma)$  increases as the correlation coefficient increases. The table also indicates that the fractiles of  $L_A(t, \gamma)$  for smaller probability of exceedance levels are sensitive to the considered spatial correlation. This could significantly affect the evaluation of the so-called ruin probability for the insurance industry, and the decision-making of risk mitigation policies. Note that the observed behavior of aggregate seismic losses are in agreement with those derived based on the consideration of correlation of the combinations of structural resistance and seismic demand for a group of structures by Hong (2000).

The above analysis is repeated but with the attenuation relations in Set-1 replaced by those in Set-2, the obtained samples of  $L_A(t, \gamma)$  are shown in Fig. 5, and the statistics of  $L_A(t, \gamma)$  are listed in Table 2. Comparison of the results shown in Figs. 4 and 5, and Table 2 indicates that overall tendencies are similar although the seismic risk by using Set-1 are slightly higher than that by using Set-2.

In all cases, the numerical results indicate that if one is interested in providing adequate probabilistic characterizations of seismic risk, that is the aggregate seismic losses at present value, one must use a sound estimate of the spatial correlation of seismic demand rather than simply assuming no correlation or

full correlation of seismic demand. Most importantly, unrealistic estimates of fractiles of  $L_A(t, \gamma)$  that corresponds to specific ruin probability levels may be obtained if an inadequate estimate of the spatial correlation is adopted.

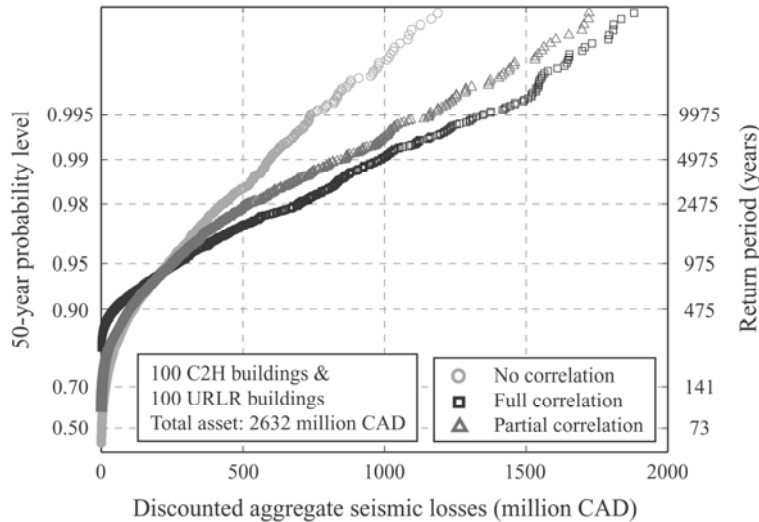


Figure 5. Discounted 50-year aggregate seismic losses plotted on the Gumbel probability paper (attenuation relation in Set-2 are adopted).

### Conclusions

A simulation-based methodology of probabilistic seismic hazard and risk assessments for a group of structures is developed. The methodology can incorporate correlations of random variables such as seismic demand, structural resistance, and damage cost explicitly. In particular, the emphasis is given to the correlation of seismic demand which is characterized by inter-event correlation and intra-event spatial correlation. The developed framework accounts for the simultaneous occurrence of structural damage and collapse of a group of structures, which result in catastrophic seismic losses due to rare but large events. Such model characteristics are of particular interest for corporate managers, city planners, and insurers who face with potential seismic risk for spatially distributed buildings in their jurisdictions. The seismic risk assessment framework based on seismic hazard modeling, damage assessment, and seismic loss estimation is illustrated.

The numerical results considering a hypothetical building inventory of 200 buildings located in western Canada suggest that the probability distribution of the aggregate seismic losses obtained by considering realistic spatial correlation is significantly different from those obtained with no correlation and full correlation. Further, the former is bounded by the latter. It is noteworthy that the expected aggregate seismic loss is independent of characteristics of the correlation of seismic demand whereas the probability distribution function of the aggregate seismic losses, therefore the higher order statistics and fractiles corresponding to the specified (ruin) probability levels, can be affected significantly by the spatial correlation of seismic demand. This fact emphasizes the importance of considering a sound estimate of the spatial correlation of seismic demand rather than simply assuming no correlation or full correlation for seismic hazard and risk assessments of a group of structures.

### Acknowledgments

The financial supports of the Natural Science and Engineering Research Council of Canada and the University of Western Ontario are gratefully acknowledged.

## References

- Adams, J. and S. Halchuk, 2003. Fourth generation seismic hazard maps of Canada: values for over 650 Canadian localities intended for the 2005 National Building Code of Canada, *Open-File 4459*, Geological Survey of Canada, Ottawa.
- Atkinson, G.M. and D.M. Boore, 2003. Empirical ground-motion relations for subduction-zone earthquakes and their application to Cascadia and other regions, *Bull. Seism. Soc. Am.* 93, 1703-1729.
- Baker, J.W., and C. A. Cornell, 2006. Correlation of response spectral values for multicomponent ground motions, *Bull. Seism. Soc. Am.* 96, 215-227.
- Barbat, A.H.S. Lagomarsino, and L. G. Pujades, 2006. Vulnerability assessment of dwelling buildings, *Assessing and managing earthquake risk*, Springer, Dordrecht, 115-158.
- Bazzurro, P. and N. Luco, 2004. Effects of different sources of uncertainty and correlation on earthquake-generated losses, in *Proc. Intl. Forum on Eng. Decision Making*, Stoos, Switzerland.
- Bommer, J.J. and H. Crowley, 2006. The influence of ground-motion variability in earthquake loss modeling, *Bull. Earthquake Eng.* 4, 231-248.
- Boore, D.M., W.B. Joyner, and T.E. Fumal, 1993. Estimation of response spectra and peak accelerations from western North American earthquakes: an interim report, *Open-File 93-509*, U.S. Geological Survey, Menlo Park, CA.
- Boore, D.M., 1997. Estimates of average spectral amplitudes at FOAKE sites, *An evaluation of methodology for seismic qualification of equipment, cable trays, and ducts in ALWR plants by use of experience data* (Appendix C), *NUREG/CR-6464 and BNL-NUREG-52500*, C1-C69.
- Federal Emergency Management Agency (FEMA), and the National Institute of Building Sciences (NIBS), 2003. HAZUS-MH: technical manual, Washington, D.C.
- Goda, K., and H.P. Hong, 2006. Optimal seismic design for limited planning time horizon with detailed seismic hazard information, *Structural Safety* 28, 247-260.
- Goda, K., and H.P. Hong, 2007. Spatial correlation of peak ground motions and response spectra, *Bull. Seism. Soc. Am.* (submitted).
- Grossi, P., 2000. Quantifying the uncertainty in seismic risk and loss estimation, *Ph.D. thesis*, Univ. of Pennsylvania, Philadelphia, PA.
- Hong, H.P., 2000. Distribution of structural collapses and optimal reliability for infrequent environmental loads, *Structural Safety* 22, 297-311.
- Hong, H.P., and P. Hong, 2006. Reliability of bilinear SDOF systems subjected to earthquake loading, in *Proc. Intl. Conference on Advances in Eng. Structures, Mechanics & Construction*, Waterloo, Springer, 711-723.
- Hong, H.P., K. Goda, and A.G. Davenport, 2006. Seismic hazard analysis: a comparative study, *Canadian J. Civil Eng.* 33, 1156-1171.
- Hong, H.P., and K. Goda, 2007. Orientation-dependent ground motion measure for seismic hazard assessment, *Bull. Seism. Soc. Am.* (accepted).
- Kawakami, H., and H. Mogi, 2003. Analyzing spatial intraevent variability of peak ground accelerations as a function of separation distance, *Bull. Seism. Soc. Am.* 93, 1079-1090.

- Kleindorfer, P.R., P. Grossi, and H.C. Kunreuther, 2005. The impact of mitigation on homeowners and insurers: an analysis of model cities, *Catastrophe modeling: a new approach to managing risk*, Springer, New York, 167-188.
- Munich Reinsurance Company of Canada (Munich Re.), 1992. A study of the economic impact of a severe earthquake in the lower mainland of British Columbia, Vancouver.
- National Research Council of Canada (NRCC), 2005. *National Building Code of Canada 2005*, Ottawa.
- Onur, T., C.E. Ventura, and W.D.L. Finn, 2005. Regional seismic risk in British Columbia – damage and loss distribution in Victoria and Vancouver, *Canadian J. Civil Eng.* 32, 361-371.
- Means, R.S., 2003. Building construction cost data 61th ed., *R.S. Means Company, Inc.*, Kingston, MA.
- Wang, M., and T. Takada, 2005. Macrospatial correlation model of seismic ground motions, *Earthquake Spectra* 21, 1137-1156.
- Wesson, R.L., and D.M. Perkins, 2001. Spatial correlation of probabilistic earthquake ground motion and loss, *Bull. Seism. Soc. Am.* 91, 1498-1515.
- Youngs, R.R., W.J. Silva, and J.R. Humphrey, 1997. Strong ground motion attenuation relationships for subduction zone earthquakes, *Seism. Res. Lett.* 68, 58-72.